IET Nanobiotechnology

Research Article

IET Journals
The Institution of Engineering and Technology

Escherichia coli bacteria detection by using graphene-based biosensor

ISSN 1751-8741
Received on 3rd February 2015
Revised on 2nd March 2015
Accepted on 15th March 2015
doi: 10.1049/iet-nbt.2015.0010
www.ietdl.org

Elnaz Akbari[1], Zolkafle Buntat[1] ✉, Abdolkarim Afroozeh[2,3], Alireza Zeinalinezhad[4], Ali Nikoukar[5]

[1]*Faculty of Electrical Engineering, Institute of High Voltage & High Current, Universiti Teknologi Malaysia, Johor Bahru 81310, Malaysia*
[2]*Jahrom Branch, Young Researchers and Elite Club, Islamic Azad University, Jahrom, Iran*
[3]*The Department General of Fars Province Education, Iran*
[4]*Chemistry Department, Anar Branch, Islamic Azad University, Anar, Iran*
[5]*Faculty of Computing, Universiti Teknologi Malaysia, Johor Bahru 81310, Malaysia*
✉ *E-mail: zolkafle@fke.utm.my*

Abstract: Graphene is an allotrope of carbon with two-dimensional (2D) monolayer honeycombs. A larger detection area and higher sensitivity can be provided by graphene-based nanosenor because of its 2D structure. In addition, owing to its special characteristics, including electrical, optical and physical properties, graphene is known as a more suitable candidate compared to other materials used in the sensor application. A novel model employing a field-effect transistor structure using graphene is proposed and the current–voltage (*I–V*) characteristics of graphene are employed to model the sensing mechanism. This biosensor can detect *Escherichia coli* (*E. coli*) bacteria, providing high levels of sensitivity. It is observed that the graphene device experiences a drastic increase in conductance when exposed to *E. coli* bacteria at 0–10^5 cfu/ml concentration. The simple, fast response and high sensitivity of this nanoelectronic biosensor make it a suitable device in screening and functional studies of antibacterial drugs and an ideal high-throughput platform which can detect any pathogenic bacteria. Artificial neural network and support vector regression algorithms have also been used to provide other models for the *I–V* characteristic. A satisfactory agreement has been presented by comparison between the proposed models with the experimental data.

1 Introduction

Escherichia coli (*E. coli*) bacteria was discovered in the human colon in 1885 and is associated with German bacteriologist Theodor Escherich. He found correlations between particular strains of the bacteria and diarrhoea and gastroenteritis in infants, which was a significant finding in the public health area, hence the change of the name of the bacteria from bacterium coli to *E. coli* in his honour [1, 2]. It must be noted that not only do most *E. coli* bacteria not cause any illness in humans, but some even act for the benefit of the human body. However, several *E. coli* strains cause infections that are not gastrointestinal disorders, but rather those of the urinary tract [3, 4].

In *E. coli* sensing, several biosensor structures have been presented, such as optical biosensors, photodiode-based sensing [5], integrate waveguide biosensors [6] electro-chemical sensing techniques [7–10] or carbon nanotubes biosensor based on field-effect transistor (FET) structure with very high bound of sensing [11–14]. Nonetheless, the greater parts of these experiments need the use of labels for detection; hence, a more clear method is required. These biosensor fabrications can be unmanageable or the limit of sensing is remarkably lower than preferred. The properties and definition of nanomaterials utilised as a part of nanobiotechnology for *E. coli* sensing are recorded in Table 1.

Here, we explain a graphene-based nanoelectronic sensor with extremely sensitive bacteria (*E. coli*) detection (10 cfu/ml). In contrast to the mentioned approaches, which are time-consuming and tedious, the graphene-based nanoelectronic offers delicate and quick estimation. This work has novel approaches because, for the first time, the effect of *E. coli* detection on graphene electrical properties is studied and formulated. Furthermore, typically, two distinct states, namely equilibrium (statistical) and non-equilibrium conditions are considered in most studies. In this research, both states have been applied in the mathematical formulation of the sensor models.

Carbon-based materials have been explored extensively to accommodate the advancing technology nowadays [15–17]. The discovery of a single atomic sheet of graphite layer or graphene by Andre Geim in 2004 has attracted much interest in the communities of research and technology because of its superb electronic properties [18–21]. Single layer graphene consists of sp^2-bonded carbon atoms arranged in the form of a hexagonal lattice (honeycomb lattice) in a two-dimensional (2D) structure comprising a thin layer of single carbon atoms [20, 22–25]. Graphene has a very high charge carrier mobility that can exceed 200 000 cm^2/Vs at room temperature. According to experimental transport measurement results, due to the extraordinary feature of high electron mobility, graphene has become an extremely attractive material for use in future nanoelectronic devices, particularly in sensor applications [26–29].

Herein, we introduce a FET biosensor modified from graphene, which shows promoted performance for measuring the bacterium. The prototype FET structures have indicated excellent performance for transistors, interconnects, electromechanical switches, infrared emitters and biosensors [30, 31]. As one can see in Fig. 1, it looks similar to the electrolyte-gated FET and a graphene channel connects the source and drain electrodes [32, 33]. When *E. coli* bacteria come into contact with the surface or edge of graphene, the amount of carrier concentration will change because of the variability of the drain–source current, which is a measurable parameter. According to the relation between conductivity and charge carrier density or carrier mobility, the adsorbed molecules change the conductivity of the grapheme [34–37].

In addition to the analytical model, artificial neural network (ANN) and support vector regression (SVR) models were also developed. ANNs can be identified as a simplified mathematical model based on the neurological structure of the human brain. The ability of ANN in determining complex relationships among variables makes this technique one of the most powerful tools for data modelling [26]. SVR is another technique in computational

Table 1 Description and properties of nanomaterials used in Nanobiotechnology for the *E. coli* detection

Material	Recognition element	Signal transduction method	Pathogen	Detection range	Refs.
quantum dots	antibody	fluorescence	*E. coli* O157:H7	106 cells/ml (PBS)	[51]
quantum dots	antibody	fluorescence	*E. coli*	10^4 cfu/ml	[51]
single- and multi-walled carbon nanotubes	aptamer	fluorescence	*E. coli*	10^3 cfu/ml	[14, 52–54]
magnetic nanoparticle	CP1	magnetic	*E. coli* O157:H7	10^4 cfu/ml (PBS-T)	[55–57]
magnetic bead/quantum dot	antibody	fluorescence	*E. coli* 0157:H7	10^3 cfu/ml (brain)	[58]
RuBpy doped silica	antibody	fluorescence	*E. coli* O157:H7	1 cell/ml (PBS)	[59]

intelligence associated with ANN and is fundamentally based on the theory of statistical learning proposed by Vapnik [1, 4, 22].

2 Experimental

The chemical vapour deposition method using ethanol was used for graphene film growing on copper foils. It was coated by a thin layer of poly-methyl methacrylate (PMMA) dissolved in chlorobenzene. Then, by using chemical etching method the graphene/PMMA was released from the copper foil. The drain and source (two electrodes) were prepared and passed through the graphene by using silver. Lastly, for electrode insulation silicon rubber was used [4].

E. coli (K12 ER2925) was bought from New England Biolab and cultured in LB (Luria Bertani) medium at 37°C. For 10^7 cfu/ml density *E. coli* production, culturing and colony counting methods were used. It was prepared for experimental work by diluting it in PBS solution (pH 7.2). The harvested *E. coli* was stored at 80°C.

The semiconductor device analyser was used for electrical measurement (Agilent, B1500A) and all measurements have been done under ambient conditions [4].

3 Proposed model

An *E. coli* bacterium in contact with a film of antibody functionalised graphene is illustrated in Fig. 1. In this configuration, to check the system response and to find the kinetics of bacteria binding, the sensor was kept in chambers with 10^5 cfu/ml of *E. coli* [4, 38]. As the higher number of *E. coli* is caught by the graphene film antibodies, the conductance of the channel increases. Operating the graphene-FET (GFET) in the p-type region with zero gate voltage confirms that the graphene conductance increases as a result of higher levels of hole density caused by the high negativity of the walls of the bacteria.

It has been approved by experimental methods that the conductance of graphene is a function of carrier density and mobility. In the other words, changes in electron density and/or charge carriers by adsorption of *E. coli* molecules or ions in graphene change the conductance [39].

We begin the modelling by carrier concentration given as [40, 41]

$$n = \int D(E) f(E) d(E) \tag{1}$$

where $f(E)$ is the Fermi dirac distribution and $D(E)$ shows density of state and can be written as [40]

$$D(E) = \frac{1}{3\pi t a_{c-c}} \frac{E}{\sqrt{E^2 - \left(E_g/2\right)^2}} \tag{2}$$

in which $a_{C-C} = 1.42$ Å represents carbon–carbon (C–C) bond length, and $t = 2.7$ eV is the nearest neighbour C–C tight binding overlap energy. E_g is the bandgap energy, which can be written

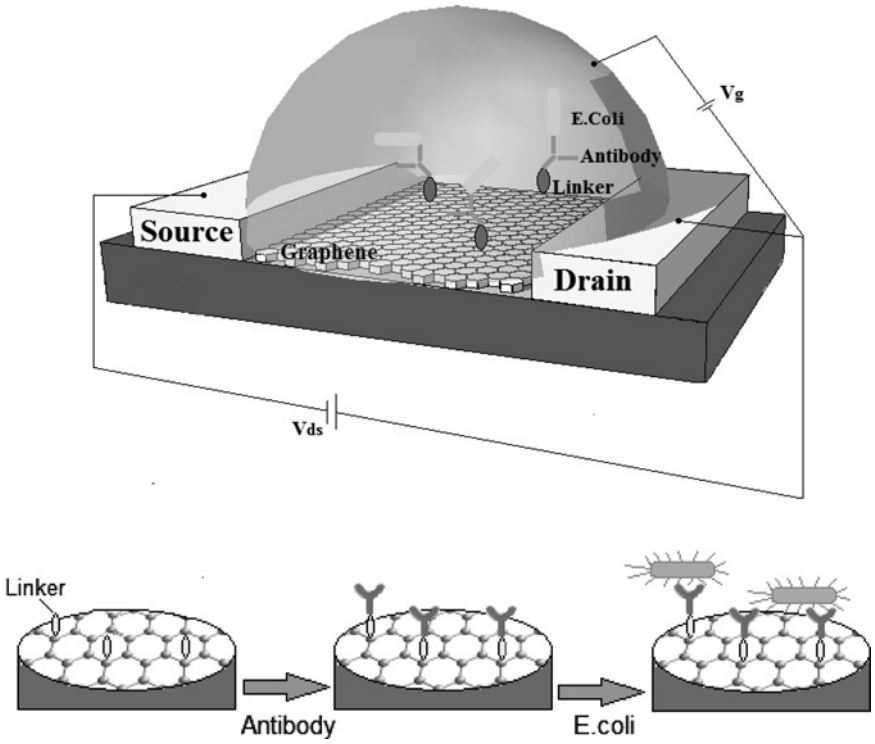

Fig. 1 *GFET for detection of E. coli*

IET Nanobiotechnol., 2015, Vol. 9, Iss. 5, pp. 273–279

for monolayer graphene as [42, 43]

$$E_g = 2\pi\sqrt{3}\left(\frac{p}{N+1} - \frac{2}{3}\right) \tag{3}$$

in which p signifies an integer number, and the Fermi dirac distribution $f(E)$ is defined as [44]

$$f(E) = \frac{1}{\exp\left(E - E_F/k_B T\right) + 1} \tag{4}$$

where E_F is the Fermi energy, K_B is the Boltzmann's constant, T is the temperature and E is the energy then the *E. coli* concentration is written as

$$n = \int \frac{1}{3\pi t a_{c-c}} \frac{E}{\sqrt{E^2 - \left(E_g/2\right)^2}} \cdot \frac{1}{\exp\left(E - E_F/k_B T\right) + 1} \cdot d(E) \tag{5}$$

The quantum capacitance is shown as [45]

$$C_q = \frac{\partial Q}{\partial V} \tag{6}$$

in which Q is the charge measured in coulombs and $\partial Q = e\,\partial n_{Total}$, e is the electron charge, $n_{Total} = n + n'$, where n is the inherent carrier concentration and n' is the amount of carrier concentration when lipid is injected.

$\partial V = \partial E/e$ is the voltage applied to the device and C_q is given as [46]

$$C_q = \frac{e\partial n_{Total}}{\partial E/e} \tag{7}$$

which becomes by a simple mathematical rearrangement

$$C_q = e^2 \frac{\partial n_{Total}}{\partial E} \tag{8}$$

Using the definition of n_{Total}, the following equation can be written for quantum capacitance

$$C_q = e^2 \frac{\partial n}{\partial E} + e^2 \frac{\partial n'}{\partial E} \tag{9}$$

The performance of the bio-sensor based on graphene nanostructure is demonstrated by its conductance characteristic. As V_g results in altering conductance of the channel, one of the parameters that has a strong influence on bio sensor conductance is *E. coli* concentration, so we can write

$$n' = \psi F_{EC} \tag{10}$$

where (F_{EC}) is the carrier concentration of *E. coli* and the control parameter is indicated by (ψ). As a result, the quantum capacitance can be written as

$$C_q = e^2 \cdot \frac{1}{3\pi t a_{c-c}} \frac{E}{\sqrt{E^2 - \left(E_g/2\right)^2}} \cdot \frac{1}{\exp\left(E - E_F/k_B T\right) + 1} + e^2 \psi \frac{\partial F_{EC}}{\partial t} \frac{\partial t}{\partial E} \tag{11}$$

The GFET conductance can be shown as follows

$$G = \left(e^2 \cdot \frac{1}{3\pi t a_{c-c}} \frac{E}{\sqrt{E^2 - \left(E_g/2\right)^2}} \cdot \frac{1}{\exp\left(E - E_F/k_B T\right) + 1} + e^2 \psi \frac{\partial F_{EC}}{\partial t} \frac{\partial t}{\partial E} \right) \cdot V_{ds} \cdot \mu_e \tag{12}$$

On the basis of the analytical model, ψ is introduced as the *E. coli* controlled parameter and shows the rate of changes in conductivity depends on *E. coli* concentration that is given by

$$\psi = aLn(F_{EC}) + b \tag{13}$$

where in the same manner constant parameters has been calculated as: $a = 57550$ and $b = 18848$.

To check their functionality, the graphene devices were kept in closed chambers with various *E. coli* concentrations to allow the bacteria to grow and multiply. The graphene devices were then washed with a phosphate-buffered saline (PBS) solution of pH 7.2 (to allow for the production of the intended final *E. coli* concentration) [4] and were electrically tested through measuring the current–voltage (I–V) characteristics with zero voltage between the solution and the gate. The corresponding I–V curves of a single graphene device before and after being exposed to *E. coli* bacteria at concentrations between 0 and 10^4 cfu/ml are illustrated in Figs. 2*a*–*f*.

The I–V characteristics of the proposed model for a biosensor based on graphene in comparison with results from experimental data have been illustrated in Figs. 2*a*–*f*. It can be observed that the charge transfer between *E. coli* (0–100 000 cfu/mol) and graphene causes the current to increase. An acceptable agreement between extracted data and the suggested model is illustrated clearly in the figures. In the proposed model, different amounts of *E. coli* concentration are shown in term of control parameter (ψ) as presented in Table 2.

Fig. 3 shows the evaluation of the rate increment in conductance of graphene affected by several bacteria concentrations.

As can be seen, concentrations of *E. coli* as low as 10 cfu/ml could be ambiguously sensed. This is several steps lower than the formerly stated approaches used by single-walled carbon nanotubes-network FETs [47], polymerase series response [48], external plasmon intensification [49]. Particularly, 10 cfu/ml created a $3.25 \pm 0.43\%$ increment in graphene-based sensor conductance ($n = 6$ devices) which relates to the existing increment of $\sim$1.17 μA at $V_{ds} = 0.2$ V (notably greater than the existing noise of (0.02 μA)). In Table 3, the validation data for the analytical model are presented.

4 ANN and SVR models

This study aims to carry out a comparative study between SVR and back-propagation ANNs to assess their characteristics and potentials in the prediction of I–V characteristics.

The proposed ANN has been developed incorporating a network comprising three layers: one input, one output and one hidden layer, and feed-forward structure has been employed for this ANN model. MATLAB software was utilised for programming and the extracted experimental data were used as the training data set as well as testing input. The values for the weights and bias are randomly chosen by the software and updated in each epoch using the back-propagation learning algorithm.

Recently, the SVR has been employed for prediction in chemical applications. In our research, we use the ε-SVR, which gives an approximate function $f(x)$ that limits the deviations from the target y_i in the training data set (i.e. $\{(x_1, y_1),\ldots,(x_l, y_L)\} \subseteq (X \times Y)^l$) not to exceed a maximum value ε and makes it as flat as possible

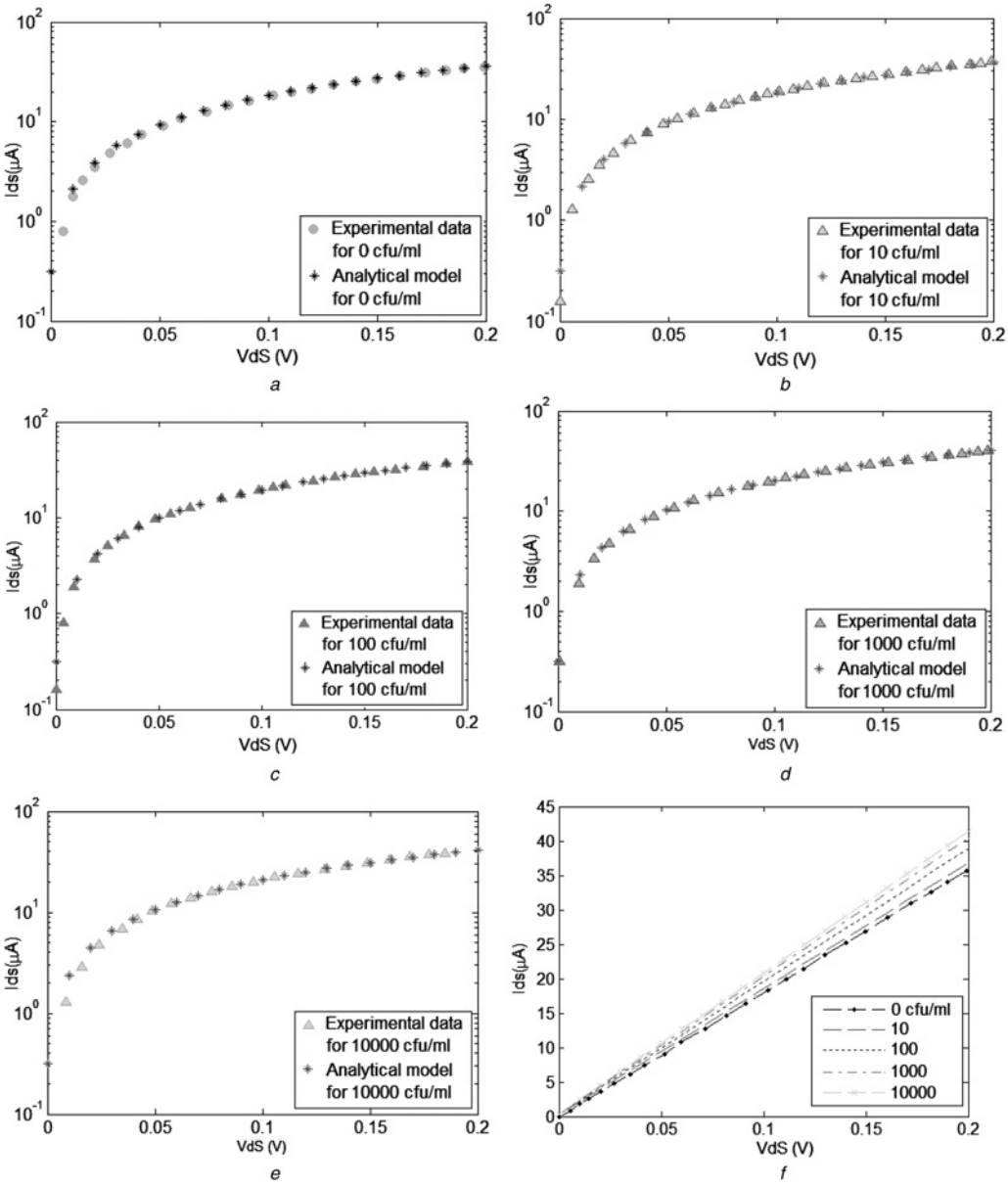

Fig. 2 *I–V characteristics for different E. coli concentrations*

[3, 38]. In other words, errors are neglected as long as they are smaller than a pre-specified value, ε. Unlike the ANN, training of the SVR includes convex optimisation in which there are no local minima [22]. A transformation function Φ is applied in the SVR algorithm to the original points to transform them from the initial input space to a feature space F of a higher dimension. In the obtained new space, a linear model is constructed corresponding to a non-linear model in the original space. Consider a simple linear problem; for this case, the transformation function is in the form of $f(x) = \langle w, \Phi(x)\rangle + b$ where $w \in X$, and $b \in \Re$. Here $\langle w, \Phi(x)\rangle$ represents the dot product of the input patterns, x in the feature space [3, 4, 28]. As a matter of fact, the support vectors are the data points which are used in the description of the searched function [20]. In the presence of noise, working with a soft margin obtained from the support vector machines (SVM) would be more plausible. This can be evidently realised by slack variables

Table 2 ψ parameter corresponding to *E. coli* concentration values

F, cfu/mol	ψ
0	0.7
10	0.72
100	0.75
1000	0.78
10 000	0.8

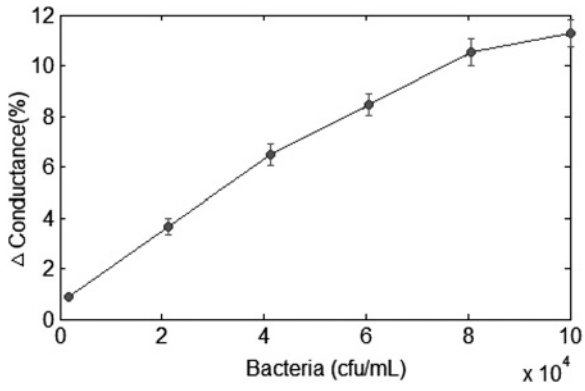

Fig. 3 *Changes in the concentration of E. coli causes varying percentages of graphene conductance*

Averages of the values read from six devices are taken for each data point and the corresponding standard errors are represented by error bars

Table 3 Validation data for analytical model at different concentrations of *E. coli*

E. coli concentration	0	10	100	1000	10 000
MSE	0.0128	0.00009	0.0008	0.0003	0.0072
R2	0.9411	0.9986	0.9915	0.9966	0.9613
Q2	0.7951	0.9979	0.9811	0.9910	0.8334
RSS	0.0913	0.0016	0.0108	0.0039	0.0429
TSS	1.5512	1.1619	1.2765	1.1479	1.1079
SSE	0.2681	0.0021	0.0182	0.0081	0.1443
PRESS	0.3178	0.0024	0.0241	0.0103	0.1846

Table 4 Selected values for ε, C and γ

Concentration, cfu/ml	ε	C	γ
0	1.9	35.6627	0.07
10	1.7	37.1314	0.09
100	1.1	38.4	0.03
1000	1.5	39.8400	0.04
10 000	1.4	38.8755	0.02

$\xi_i^-, \xi_i^+ \geq 0$ with which the mathematical formulation can be extended in convex optimisation [22]

$$\frac{1}{2}||W||^2 + C\sum_{i=1}^{l}(\xi_i^+ + \xi_i^-) \tag{14}$$

In order to ensure flatness, the equation above must be minimised by $\|W\|^2 = \langle w, w\rangle$ and applying the constraints

$$(w \cdot \phi(x_i)) + b - y_i = \varepsilon + \xi_i^- y_i - (w \cdot \phi(x_i)) - b \leq \varepsilon + \xi_i^+$$

[20, 22]. Constant C determines the trade-off between flatness and the amount of outliers of the ε-tube, which is handled in this study with the ε-intensive loss function [50]

$$|\xi|_\varepsilon := \begin{cases} 0 & \text{if } |\xi| \leq \varepsilon \\ |\xi| \leq \varepsilon & \text{otherwise} \end{cases} \tag{15}$$

Employing the kernel function, one can derive a solution for the original regression problem, without the need to consider the transformation $\Phi(x)$ applied to the data explicitly. In this study, we have implemented radial basis functions (RBF). The accuracy of

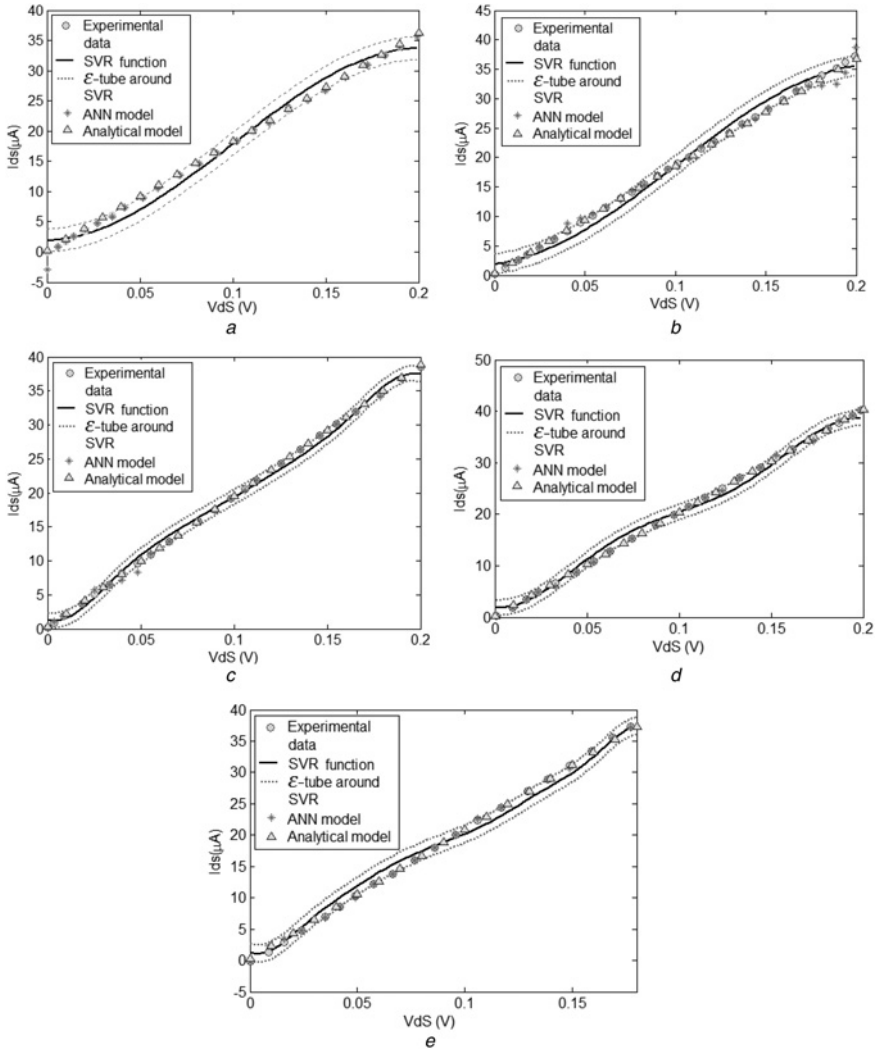

Fig. 4 *I–V characteristics of anti E. coli antibody in different concentrations of E. coli*

a 0 cfu/ml concentration of *E. coli*
b 10 cfu/ml concentration of *E. coli*
c 100 cfu/ml concentration of *E. coli*
d 1000 cfu/ml concentration of *E. coli*
e 10 000 cfu/ml concentration of *E. coli*

Table 5 Validation data for SVR and ANN models at different concentrations of *E. coli*

E. coli concentration	SVR					ANN				
	0	10	100	1000	10 000	0	10	100	1000	10 000
MSE	0.0066	0.0020	0.0002	0.0007	0.0007	0.0011	0.0015	0.0004	0.0001	0.0002
R2	0.9840	0.9932	0.9981	0.9959	0.9966	0.9973	0.9952	0.9985	0.9993	0.9990
Q2	0.9358	0.9794	0.9965	0.9912	0.9905	0.9865	0.9787	0.9947	0.9986	0.9965
RSS	0.0434	0.0225	0.0040	0.0103	0.0064	0.0054	0.0114	0.0031	0.0017	0.0019
TSS	2.7137	3.3204	2.1627	2.5432	1.8692	2.0027	2.3925	2.1214	2.3037	1.8668
SSE	0.1450	0.0685	0.0058	0.0183	0.0142	0.0221	0.0428	0.0096	0.0027	0.0053
PRESS	0.1742	0.0594	0.0076	0.0224	0.0178	0.0271	0.0510	0.0113	0.0033	0.0066

the model for the ε-SVR with RBF kernel function is dependent upon the parameters ε, C and γ. As previously mentioned, the accuracy of the approximated function is determined by the magnitude of ε. For values of ε larger than the range of target data, expecting accurate results is a little over-optimistic. One can expect over-fitting for zero ε. Thus, ε must be chosen so that it somehow reflects the data. The values of insensitivity function ε, and parameters C and γ were selected by trial and error method and are tabulated in Table 4.

In summary, the ANN model that we employed comprises a multi-layer feed forward neural network and the SVM model developed is a SVR with radial kernel function. The analysis considered modelling of *I–V* characteristics in graphene-based biosensor. The results are provided in Figs. 4*a–e*, where the results from ANN and SVR are compared with those from the extracted experimental data. Results of this comparison indicate that the ANN significantly outperformed SVR in predicting the *I–V* characteristics of the proposed biosensor model. While more investigation is necessary to draw definite conclusions regarding the advantages of ANN over SVR, based on the investigations conducted in this study, it was found that ANN is a viable alternative for SVR in modelling the *I–V* characteristics in graphene-based *E. coli* sensor.

Model validation parameters for SVR and ANN are tabulated in Table 5. As observed from these validation data, it is evident that the ANN model can best fit the experimental data and thus predict the sensor behaviour.

5 Conclusion

Three different models were developed using ANN, SVR and analytical method to characterise the *I–V* relation of a graphene-based sensor for *E. coli* bacteria. The graphene component shows measurable sensitivity when in contact with *E. coli* as its conductance changes. Hence, this behaviour is proposed to be used in the detection of this type of bacteria. A bacteria concentration control parameter (ψ) is introduced in the derivation of the analytical model and is calculated iteratively. In synopsis, the created sensor is label-free, rapid, extremely sensitive and selective biosensor for detection of bacteria *E. coli*. A very low sensing limit of 10 cfu/ml can be reached. Comparison between the results obtained from the three models shows that ANN is able to provide more accurate estimations. With the aid of the proposed models, a realistic understanding of the biosensor performance under exposure to *E. coli* can be gained, minimising the need for empirical experiments.

6 Acknowledgments

The authors would like to thank the Ministry of Higher Education (MOHE) Malaysia (grant vot. no. 4F382) and the Universiti Teknologi Malaysia (grant vot. nos. 03H86 and 04H40) for the financial support received during the investigation.

7 References

1 Anthony, M.: 'Computational learning theory' (Cambridge University Press, Cambridge, 1997)
2 Wittstock, A., Biener, J., Erlebacher, J.: 'Nanoporous gold: from an ancient technology to a high-tech material', (Royal Society of Chemistry, London, 2012)
3 Stahlbock, R., Lessmann, S.: 'Potential von support vektor maschinen im analytischen customer relationship management' (Universität Hamburg, Hamburg, Arbeitspapier, 2004)
4 Huang, Y., Dong, X., Liu, Y., Li, L.-J., Chen, P.P.: 'Graphene-based biosensors for detection of bacteria and their metabolic activities', *J. Mater. Chem.*, 2011, **21**, (33), pp. 12358–12362
5 Song, J.M., Kwon, H.T.: 'Photodiode array on-chip biosensor for the detection of E. coli O157: H7 pathogenic bacteria'. Biosensors and Biodetection, Springer, 2009, pp. 325–335
6 Zhu, P., Shelton, D.R., Karns, J.S., *et al.*: 'Detection of water-borne *E. coli* O157 using the integrating waveguide biosensor', *Biosens. Bioelectron.*, 2005, **21**, (4), pp. 678–683
7 Zhang, X., Geng, P.P., Liu, H., *et al.*: 'Development of an electrochemical immunoassay for rapid detection of *E. coli* using anodic stripping voltammetry based on Cu@ Au nanoparticles as antibody labels', *Biosens. Bioelectron.*, 2009, **24**, (7), pp. 2155–2159
8 Liao, J.C., Mastali, M., Li, Y., *et al.*: 'Development of an advanced electrochemical DNA biosensor for bacterial pathogen detection', *J. Mol. Diagn.*, 2007, **9**, (2), pp. 158–168
9 Yang, L., Bashir, R.: 'Electrical/electrochemical impedance for rapid detection of foodborne pathogenic bacteria', *Biotechnol. Adv.*, 2008, **26**, (2), pp. 135–150
10 Chang, L., Liu, C., He, Y., Xiao, H., Cai, X.: 'Small-volume solution current-time behavior study for application in reverse iontophoresis-based non-invasive blood glucose monitoring', *Sci. Chin. Chem.*, 2011, **54**, (1), pp. 223–230
11 Vashist, S.K., Zheng, D., Al-Rubeaan, K., Luong, J.H., Sheu, F.-S.: 'Advances in carbon nanotube based electrochemical sensors for bioanalytical applications', *Biotechnol. Adv.*, 2011, **29**, (2), pp. 169–188
12 García-Aljaro, C., Cella, L.N., Shirale, D.J., *et al.*: 'Carbon nanotubes-based chemiresistive biosensors for detection of microorganisms', *Biosens. Bioelectron.*, 2010, **26**, (4), pp. 1437–1441
13 Zhang, X., Wang, D., Yang, D., Li, S., Shen, Z.: 'Electronic detection of *Escherichia coli* O157：H7 using single-walled carbon nanotubes field-effect transistor biosensor', *Engineering*, 2013, **4**, (10), p. 94
14 Villamizar, R.A., Maroto, A., Rius, F.X., Inza, I., Figueras, M.J.: 'Fast detection of *Salmonella infantis* with carbon nanotube field effect transistors', *Biosens. Bioelectron.*, 2008, **24**, (2), pp. 279–283
15 Balabin, R.M., Lomakina, E.I.: 'Support vector machine regression (SVR/LS-SVM) – an alternative to neural networks (ANN) for analytical chemistry? Comparison of nonlinear methods on near infrared (NIR) spectroscopy data', *Analyst*, 2011, **136**, (8), pp. 1703–1712
16 Goh, M., Pumera, M.: 'Graphene-based electrochemical sensor for detection of 2, 4, 6-trinitrotoluene (TNT) in seawater: the comparison of single-, few-, and multilayer graphene nanoribbons and graphite microparticles', *Anal. Bioanal. Chem.*, 2011, **399**, (1), pp. 127–131
17 Akbari, E., Arora, V.K., Enzevaee, A., Ahmadi, M.T., Khaledian, M., Yusof, R.: 'Gas concentration effects on the sensing properties of bilayer graphene'. Plasmonics, 2014, pp. 1–6
18 Yuan, W., Shi, G.: 'Graphene-based gas sensors', *J. Mater. Chem. A*, 2013, **1**, (35), pp. 10078–10091
19 Wang, Q., Arash, B.: 'A review on applications of carbon nanotubes and graphenes as nano-resonator sensors', *Computat. Mater. Sci.*, 2014, **82**, pp. 350–360
20 Gunn, S.R.: 'Support vector machines for classification and regression'. ISIS technical report, 1998, vol. 14
21 Nguyen, H.B., Nguyen, V.C., Nguyen, V.T., *et al.*: 'Development of the layer-by-layer biosensor using graphene films: application for cholesterol determination', *Adv. Nat. Sci., Nanosci. Nanotechnol.*, 2013, **4**, (1), p. 015013
22 Smola, A.J., Schölkopf, B.: 'A tutorial on support vector regression', *Stat. Comput.*, 2004, **14**, (3), pp. 199–222
23 Novoselov, K.S., Fal, V., Colombo, L., Gellert, P.P., Schwab, M., Kim, K.: 'A roadmap for graphene', *Nature*, 2012, **490**, (7419), pp. 192–200
24 Pumera, M., Polsky, R., Banks, C.: 'Graphene in analytical science', *Anal. Bioanal. Chem.*, 2014, **406**, (27), pp. 6883–6884
25 Nguyen, H.B., Nguyen, V.C., Nguyen, V.T., *et al.*: 'Graphene patterned polyaniline-based biosensor for glucose detection', *Adv. Nat. Sci., Nanosci. Nanotechnol.*, 2012, **3**, (2), p. 025011

26 Specht, D.F.: 'A general regression neural network', *IEEE Trans. Neural Netw.*, 1991, **2**, (6), pp. 568–576
27 Falkovsky, L.: 'Physical properties of graphene', *Usp. Fizicheskikh Nauk*, 2012, **182**, (11), pp. 1223–1234
28 Schölkopf, B., Burges, C.J., Smola, A.J.: 'Advances in kernel methods: support vector learning' (MIT press, 1999)
29 Liu, Z., Liu, B., Ding, J., Liu, J.: 'Fluorescent sensors using DNA-functionalized graphene oxide', *Anal. Bioanal. Chem.*, 2014, **406**, (27), pp. 6885–6902
30 Foxe, M., Lopez, G., Childres, I., *et al*.: 'Detection of ionizing radiation using graphene field effect transistors'. IEEE Nuclear Science Symp. Conf. Record, Orlando, Florida, 2009, vols 1–5, pp. 90–95
31 Ohno, Y., Maehashi, K., Matsumoto, K.: 'Graphene field-effect transistors for label-free biological sensors'. 2010 IEEE Sensors, 2010, pp. 903–906
32 Hasegawa, M., Hirayama, Y., Ohno, Y., Maehashi, K., Matsumoto, K.: 'Characterization of reduced graphene oxide field-effect transistor and its application to biosensor', *Jpn. J. Appl. Phys.*, 2014, **53**, (S15), p. 05FD05
33 Schwierz, F.: 'Graphene transistors', *Nat Nano*, 2010, **5**, (7), pp. 487–496
34 Neto, A.C., Guinea, F., Peres, N., Novoselov, K.S., Geim, A.K.: 'The electronic properties of graphene', *Rev. Modern Phys.*, 2009, **81**, (1), p. 109
35 Fang, M., Wang, K., Lu, H., Yang, Y., Nutt, S.: 'Covalent polymer functionalization of graphene nanosheets and mechanical properties of composites', *J. Mater. Chem.*, 2009, **19**, (38), pp. 7098–7105
36 North, S., Lock, E., Taitt, C., Walton, S.: 'Critical aspects of biointerface design and their impact on biosensor development', *Anal. Bioanal. Chem.*, 2010, **397**, (3), pp. 925–933
37 Caucheteur, C., Guo, T., Albert, J.: 'Review of plasmonic fiber optic biochemical sensors: improving the limit of detection', *Anal. Bioanal. Chem.*, 2015, pp. 1–15. doi: 10.1007/s00216-014-8411-6
38 Welling, M.: 'Support vector regression' (Department of Computer Science, University of Toronto, Toronto, Kanada, 2004)
39 Ahmadi, M.T., Johari, Z., Amin, N.A., Fallahpour, A.H., Ismail, R.: 'Graphene nanoribbon conductance model in parabolic band structure', *J. Nanomater.*, 2010. doi: 10.1155/2010/753738
40 Lundstrom, M., Guo, J.: 'Nanoscale transistors: device physics, modeling and simulation' (Springer Science & Business Media, 2006)
41 Marulanda, J.M., Srivastava, A.: 'Carrier density and effective mass calculations in carbon nanotubes', *Phys. Status Solidi (b)*, 2008, **245**, (11), pp. 2558–2562
42 Wong, H.-S.P.P., Akinwande, D.: 'Carbon nanotube and graphene device physics' (Cambridge University Press, 2010)
43 Ismail, R., Ahmadi, M.T., Anwar, S.: 'Advanced nanoelectronics' (CRC Press, 2012)
44 Datta, S.: 'Quantum transport: atom to transistor' (Cambridge University Press, 2005)
45 Xia, J., Chen, F., Li, J., Tao, N.: 'Measurement of the quantum capacitance of graphene', *Nat. Nanotechnol.*, 2009, **4**, (8), pp. 505–509
46 Shylau, A., Kłos, J., Zozoulenko, I.: 'Capacitance of graphene nanoribbons', *Phys. Rev. B*, 2009, **80**, (20), p. 205402
47 Dong, X., Long, Q., Wang, J., Chan-Park, M.B., Huang, Y., Huang, W., Chen, P.P.: 'A graphene nanoribbon network and its biosensing application', *Nanoscale*, 2011, **3**, (12), pp. 5156–5160
48 Taylor, A.D., Ladd, J., Yu, Q., Chen, S., Homola Jiang, S.: 'Quantitative and simultaneous detection of four foodborne bacterial pathogens with a multi-channel SPR sensor', *Biosens. Bioelectron.*, 2006, **22**, (5), pp. 752–758
49 Wang, Y., Ye, Z., Ying, Y.: 'New trends in impedimetric biosensors for the detection of foodborne pathogenic bacteria', *Sensors*, 2012, **12**, (3), pp. 3449–3471
50 Müller, K.-R., Smola, A.J., Rätsch, G., Schölkopf, B., Kohlmorgen, J., Vapnik, V.: 'Predicting time series with support vector machines'. Artificial Neural Networks – ICANN'97, Springer, 1997, pp. 999–1004
51 Tully, E., Hearty, S., Leonard, P.P., O'Kennedy, R.: 'The development of rapid fluorescence-based immunoassays, using quantum dot-labelled antibodies for the detection of *Listeria monocytogenes* cell surface proteins', *Int. J. Biol. Macromol.*, 2006, **39**, (1), pp. 127–134
52 Cella, L.N., Chen, W., Myung, N.V., Mulchandani, A.: 'Single-walled carbon nanotube-based chemiresistive affinity biosensors for small molecules: ultrasensitive glucose detection', *J. Am. Chem. Soc.*, 2010, **132**, (14), pp. 5024–5026
53 Lei, J., Ju, H.: 'Nanotubes in biosensing', *Interdiscip. Rev., Nanomed. Nanobiotechnol.*, 2010, **2**, (5), pp. 496–509
54 Cheng, Y., Liu, Y., Huang, J., *et al*.: 'Amperometric tyrosinase biosensor based on Fe 3 O 4 nanoparticles-coated carbon nanotubes nanocomposite for rapid detection of coliforms', *Electrochim. Acta*, 2009, **54**, (9), pp. 2588–2594
55 So, H.M., Park, D.W., Jeon, E.K., *et al*.: 'Detection and titer estimation of *Escherichia coli* using aptamer-functionalized single-walled carbon-nanotube field-effect transistors', *Small*, 2008, **4**, (2), pp. 197–201
56 Liébana, S., Lermo, A., Campoy, S., Barbé, J., Alegret, S., Pividori, M.I.: 'Magneto immunoseparation of pathogenic bacteria and electrochemical magneto genosensing of the double-tagged amplicon', *Anal. Chem.*, 2009, **81**, (14), pp. 5812–5820
57 Mujika, M., Arana, S., Castano, E., *et al*.: 'Magnetoresistive immunosensor for the detection of *Escherichia coli* O157: H7 including a microfluidic network', *Biosens. Bioelectron.*, 2009, **24**, (5), pp. 1253–1258
58 Yang, L., Li, Y.: 'Simultaneous detection of *Escherichia coli* O157: H7 and *Salmonella typhimurium* using quantum dots as fluorescence labels', *Analyst*, 2006, **131**, (3), pp. 394–401
59 Su, X.-L., Li, Y.: 'Quantum dot biolabeling coupled with immunomagnetic separation for detection of *Escherichia coli* O157: H7', *Anal. Chem.*, 2004, **76**, (16), pp. 4806–4810